

1 Towards a kinetic-based probabilistic time geography

2

3 Jed A. Long^{1*}, Trisalyn A. Nelson¹, Farouk S. Nathoo²

4

5 ¹Spatial Pattern Analysis & Research Lab

6 Department of Geography, University of Victoria

7

8 ²Department of Mathematics & Statistics, University of Victoria

9

10 *Corresponding author email: jlong@uvic.ca

11

12

Pre-print of published version.

Reference:

Long, JA, TA Nelson, and FS Nathoo. 2010. Towards a kinetic-based probabilistic time geography. *International Journal of Geographical Information Science*. 28(5). 855-874.

DOI:

<http://dx.doi.org/10.1080/13658816.2013.818151>

Disclaimer:

The PDF document is a copy of the final version of this manuscript that was subsequently accepted by the journal for publication. The paper has been through peer review, but it has not been subject to any additional copy-editing or journal specific formatting (so will look different from the final version of record, which may be accessed following the DOI above depending on your access situation).

13

1 **Abstract**

2 Time geography represents a powerful framework for quantitative analysis of individual
3 movement. Time geography effectively delineates the space-time boundaries of possible
4 individual movement by characterizing movement constraints. The goal of this paper is to
5 synchronize two new ideas, probabilistic time geography and kinetic-based time
6 geography, to develop a more realistic set of movement constraints that consider
7 movement probabilities related to object kinetics. Using random-walk theory, the existing
8 probabilistic time geography model characterizes movement probabilities for the space-
9 time cone using a normal distribution. The normal distribution has a symmetric
10 probability density function and is an appropriate model in the absence of skewness –
11 which we relate to an object’s initial velocity. Moving away from a symmetric
12 distribution for movement probabilities, we propose the use of the skew-normal
13 distribution to model kinetic-based movement probabilities, where the degree and
14 direction of skewness is related to movement direction and speed. Following a
15 description of our model, we use a set of case-studies to demonstrate the skew-normal
16 model: a random walk, a correlated random walk, wildlife data, cyclist data, and athlete
17 movement data. Our results show that for objects characterized by random movement
18 behavior the existing model performs well, but for object movement with kinetic
19 properties (e.g., athletes), the proposed model provides a substantial improvement. Future
20 work will look to extend the proposed probabilistic framework to the space-time prism.
21

1 **1 – Introduction**

2 Over the past decade there has been rekindled interest in using ideas from
3 Hägerstrand’s (1970) time geography (Figure 1) in quantitative geographic analysis
4 (Kwan 1998, 2004, Lenntorp 1999, Miller 2003). This resurgence is largely due to
5 availability of movement data, obtained using various methods for tracking individual
6 level movements. Concepts from time geography are now routinely used as an analytic
7 framework for quantitative movement analysis (Lenntorp 1999). Supported by recent
8 developments presenting rigorous mathematical definitions for time geography (Miller
9 2005), increasingly sophisticated quantitative analyses of movement data are emerging.
10 For example, Delafontaine et al. (2011) have introduced algorithms for incorporating
11 physical barriers and obstacles into quantitative time geographic analysis.

12 < approximate location Figure 1 >

13 Object kinetics, defined by an objects current speed and direction of movement,
14 along with acceleration, can similarly influence movement opportunities defined by time
15 geography (Kuijpers *et al.* 2011). For instance, in classical time geography, movement
16 boundaries are calculated with the unrealistic expectation that an object can make
17 instantaneous changes in velocity. With object kinetics (and other physical constraints)
18 ignored, time geographic structures (i.e., the space-time cone and space-time prism)
19 substantially overestimate movement opportunities. Kuijpers et al. (2011) have quantified
20 the influence of object kinetics (from velocity and acceleration) on time geographic
21 boundaries, termed *kinetic-based time geography*. Consideration of object kinetics
22 provides a more realistic representation of time geography’s boundaries, as kinetic-based

1 time geography will exclude locations in space-time not accessible based on an
2 individual's kinetic movement abilities.

3 As a quantitative framework, time geography (and kinetic-based time geography)
4 is used to characterize the space-time boundaries on object movement, delineating
5 locations in space and time as either accessible or not. Such a binary definition (i.e.,
6 accessible, not accessible) of time geography does not account for unequal movement
7 probabilities within time geographic structures (e.g., those in Figure 1). Unequal
8 movement probabilities are a result of locations and paths that are more likely to be
9 visited than others, for instance due to shorter, more direct movement routes.

10 Several approaches have been proposed to model movement probabilities within
11 time geographic volumes (Miller and Bridwell 2009, Winter 2009, Downs 2010),
12 determining, for instance, the *probability* an object will be found at a given location in
13 space and time. Such a model for modeling movement probabilities is termed
14 *probabilistic time geography*, which quantifies variation in movement probabilities in
15 time geography (Winter and Yin 2010, 2011). With the current probabilistic models,
16 calculations typically assume random movement (i.e., random walks), resulting in the use
17 of a bivariate normal distribution for modeling potential movements in space. A random
18 movement assumption has been used extensively in wildlife movement models,
19 especially with coarser tracking intervals (Turchin 1998, Codling *et al.* 2008). Assuming
20 random movement is a limitation, as most objects move non-randomly with directed,
21 linear movements and often revisit specific locations with regularity (Gonzalez *et al.*
22 2008).

1 Kuijpers et al. (2011) identify several lingering questions in terms of kinetic-
2 based time geography, the first of which is quantifying unequal movement probabilities
3 in kinetic time geography structures, much like probabilistic time geography. The
4 objective of this research is to develop a model for quantifying movement probabilities
5 for kinetic-based time geography. We generalize the current model for probabilistic time
6 geography, proposed by Winter & Yin (2010, 2011), to account for an object's initial
7 velocity. The skew-normal distribution is proposed in place of the normal distribution
8 used in Winter & Yin to model future movement probabilities in the space-time cone
9 building upon previous attempts at factoring object kinetic properties into movement
10 uncertainty models (Prager and Yu 2005) and interpolation algorithms (Yu and Kim
11 2006).

12 The paper is organized as follows. We introduce and develop the proposed skew-
13 normal model in section 2, followed by a short discussion of the model. Section 3
14 outlines a case study, with five different datasets (a random walk, a correlated random
15 walk, wildlife data, cyclist data, and athlete data), used to compare the skew-normal
16 model against the existing probabilistic time geography model from Winter & Yin. In
17 section 4, we discuss case-study results and model limitations, followed by some
18 potential applications of the proposed model. Finally, with section 5, we conclude with
19 remarks on the impact of this work along with some areas for future research.

20 **2 – Model Development**

21 *2.1 - Model Derivation – One Dimension*

22 We will first demonstrate the concept using the 1-Dimensional situation (i.e., an
23 object moving along a straight line), where an object at a moment in time (t), located at

1 point x_t , moves with some velocity (v_t). As in traditional time geography, the object has a
2 maximum travelling velocity parameter (v_{max}). The goal of the proposed model is to
3 derive future movement probabilities at time $t + \Delta t$ that include consideration of object
4 kinetics, defined here simply as a function of its current velocity v_t (see Figure 2).

5 < approximate location Figure 2 >

6 To be a candidate, the model should satisfy three general characteristics in order
7 to relate to object movement. First, the candidate model should revert back to the normal
8 model proposed by Winter & Yin (2010, 2011) in the absence of kinetic properties.
9 Reducing to the normal model in the absence of initial kinetics seems reasonable, as
10 movement in any direction should be equally probable. Second, the shift in the
11 probability mass should be proportional to the objects current velocity (as demonstrated
12 in Figure 2). Here, interpretation of the initial kinetic properties may differ based on
13 application, allowing flexibility in model development. Finally, the mode of the resultant
14 distribution should be identifiable. The mode of the resulting distribution relates clearly
15 to the most probable location of future movement, which can be used as an expectation in
16 more formal analysis and model goodness-of-fit testing.

17 A candidate model that satisfies the aforementioned properties, is the skew-
18 normal distribution (Azzalini 1985) which we propose as a generalization of the normal
19 probability density function (pdf) from Winter & Yin (2010, 2011). Thus in order to
20 develop the model in the one-dimensional case, we are interested in modeling the
21 movement possibilities of an object in a probabilistic fashion using a univariate skew-
22 normal pdf (denoted SN_1) which takes the following form (Azzalini 1985):

23
$$f(x) = \frac{2}{\omega} \phi\left(\frac{x - \xi}{\omega}\right) \cdot \Phi\left(\alpha \left(\frac{x - \xi}{\omega}\right)\right) \quad [1]$$

1 Where the functions $\phi(\cdot)$ and $\Phi(\cdot)$ are the pdf and cumulative distribution function
 2 respectively of the standard normal distribution. The SN₁ model requires the selection of
 3 three parameters that govern the location ($\zeta \in \mathbb{R}$), scale ($\omega \in \mathbb{R}^+$), and shape ($\alpha \in \mathbb{R}$) of
 4 the SN₁ pdf. Given its form, equation [1] can be expressed alternatively as:

$$5 \quad f(x) = \frac{1}{\omega\pi} e^{-\frac{(x-\zeta)^2}{2\omega^2}} \cdot \int_{-\infty}^{\alpha\left(\frac{x-\zeta}{\omega}\right)} e^{-\frac{t^2}{2}} dt \quad [2]$$

6 Following Azzalini (1985) and Arellano-Valle & Azzalini (2008), an alternative
 7 parameterization may be used to represent the pdf in terms of the first three moments of
 8 the distribution (i.e., mean $-\mu$, variance $-\sigma^2$, and skewness $-\gamma$) with respect to ζ , ω , and
 9 α . Using measurable object movement properties, and some existing theory from
 10 probabilistic time geography (Winter & Yin, 2010; 2011) we will build a probabilistic
 11 model for object movement that considers object velocity using the SN₁ distribution. To
 12 do so we will work with the alternative parameterization (Azzalini 1985), to relate known
 13 movement properties to SN₁ parameters. A system composed of three non-linear
 14 equations (in ζ , ω , and α) is used to derive a realistic SN₁ parameterization to
 15 probabilistically define object movement possibilities that incorporates object velocity.
 16 As will be seen, it is advantageous to investigate the three alternate parameters in reverse
 17 order starting first with γ .

18 The third moment (γ) of a SN₁ can be related to the shape parameter (α) directly
 19 by:

$$20 \quad \gamma = \frac{4 - \pi}{2} \frac{(\delta \sqrt{2/\pi})^3}{(1 - 2\delta^2/\pi)^{3/2}}, \quad \text{where } \delta = \frac{\alpha}{\sqrt{1 + \alpha^2}} \quad [3]$$

1 We wish to restrict γ to $[-1, 1]$ as the maximum theoretical skewness is ~ 1 , obtained by
 2 setting $\delta = 1$ in [3]. Further, the goal is to relate γ to the properties of object motion,
 3 which will vary depending on the object type and context (Prager and Yu 2005). We
 4 propose a model where the skewness of the SN_1 (modeled via parameter γ), is calculated
 5 directly from the object's initial velocity, and is relative to the object's maximum
 6 velocity. A simple formulation for γ which satisfies the above conditions is the ratio of v_t
 7 to v_{max} .

$$8 \quad \gamma = - \frac{v_t}{v_{max}} \quad [4]$$

9 The negative sign in [4] reflects the fact that if initial velocity is in the positive direction,
 10 the direction of the skewness is negative (i.e., if v_t is positive the bulk of the distribution
 11 should be in the positive direction). By substituting [4] into [3] one can solve for the
 12 shape parameter α , which will have a unique, real-valued solution.

13 The second moment (σ^2) can be expressed in terms of the shape parameter (α –
 14 which has already been identified) and the scale parameter (ω) by:

$$15 \quad \sigma^2 = \omega^2 \left(1 - \frac{2\delta^2}{\pi} \right), \quad \text{where } \delta = \frac{\alpha}{\sqrt{1 + \alpha^2}} \quad [5]$$

16 We are motivated to use what has already been shown from probabilistic time geography
 17 (Winter & Yin, 2010; 2011) to relate the variance of the SN_1 to time geography
 18 properties. Winter and Yin (2010) suggest that the variance of a normal pdf relates
 19 directly to the maximum extent of the space-time cone volume (i.e., $v_{max} \times \Delta t$) through
 20 the simple idea that at its maximum extent, the pdf is zero. Following Winter and Yin
 21 (2010) we can approximate that the pdf is 0 at 3σ (i.e., by definition 99.7 % of the normal

1 pdf volume is within three standard deviations of the mean). We adopt an identical
 2 assumption for use with the SN_1 pdf; that is:

$$3 \quad 3\sigma = v_{max} \times \Delta t \quad [6]$$

4 By substituting the solved values for σ [6], and α [3], into [5], one can obtain a quadratic
 5 equation in terms of ω . Since the scale parameter (ω) is strictly positive, of interest is the
 6 positive solution. This leaves only the remaining parameter (ξ) to identify.

7 Unfortunately, the first moment (μ) of a SN_1 is not very meaningful in the context
 8 of object movement. However, the *mode* of a SN_1 (denoted as $\hat{\mu}$) can be used to model
 9 the most probable location of future movement[†]. For a SN_1 pdf $\hat{\mu}$ is not available in
 10 analytic form, but can be found by solving for the root of the first derivative of the SN_1
 11 pdf (Gupta & Gupta, 2004), that is we must solve:

$$12 \quad f'(x) = \frac{d}{dx} \left[\frac{2}{\omega} \phi \left(\frac{x - \xi}{\omega} \right) \cdot \Phi \left(\alpha \left(\frac{x - \xi}{\omega} \right) \right) \right] = 0 \quad [7]$$

13 The SN_1 pdf is unimodal and therefore [7] possesses a single, unique root. Unfortunately,
 14 [7] cannot be easily represented in an analytical form, requiring the use of numerical
 15 methods to obtain the root. It is intuitive enough to visualize the most probable location
 16 of future movement occurring at the mode (e.g., Figure 1b). We propose a simple model
 17 where $\hat{\mu}$ is a function of the objects current location (x_t), current velocity (v_t), and the
 18 time difference into the future (Δt).

$$19 \quad \hat{\mu} = x_t + (v_t \times \Delta t) \quad [8]$$

[†] Here we assume, as in physics, that moving objects tend to continue their motion unless acted on by other forces. That is, it is *most* probable that the object does not change speed or direction.

1 More sophisticated formulations for $\hat{\mu}$ may be warranted that consider the ratio of v_t to
2 v_{max} , the magnitude of Δt , and the objects acceleration. By substituting $\hat{\mu}$ (obtained from
3 [8]) for x into [7], along with the previously computed values for ω and α , one can obtain
4 a function for the single remaining unknown – ζ , which can be solved using numerical
5 methods.

6 In summary, using known values for x_t , v_t , Δt , and v_{max} , we derive a system of
7 three non-linear equations to solve for SN₁ parameters α , ω , and ζ using the following
8 steps.

- 9 1. Substitute [4] into [3] in order to explicitly solve for the shape parameter – α .
- 10 2. Substitute α and [6] into [5] and solve for the scale parameter – ω , where $\omega > 0$.
- 11 3. Substitute values for α and ω , along with the computed value for $\hat{\mu}$ from [8] into
12 [7], to solve for the location parameter – ζ .

13 Recall that in step 3 this procedure requires that [7] be solved numerically as it is not
14 analytically tractable. Solving of the above system of non-linear equations is done in the
15 mathematical software Maple (Maplesoft, Waterloo, Ontario). The resulting values for
16 parameters ζ , ω , and α can be used to model the future movement possibilities for the
17 object based on the SN₁ model. We have used the ‘sn’ package available in R (R
18 Development Core Team 2012) to build and sample from skew-normal distributions.

19 2.2 - *Extending the Model – Two Dimensions (Spatial Movements)*

20 Extension of the univariate model to two dimensions for application with
21 movement data recorded in the spatial plane (i.e., with XY coordinates) requires the
22 consideration of several key properties. When an object exhibits kinetic effects, this
23 movement is associated with a direction in the spatial plane. Consider this direction to be

1 the axis-of-movement (AoM), and thus there is an associated axis perpendicular to the
2 movement (A+M). In practice it may be useful to examine movement based on these two
3 axes using rotations of the natural (XY) coordinates (Figure 3). These two newly defined
4 axes (AoM and A+M) are useful properties for developing and comparing candidate
5 models.

6 < approximate location Figure 3 >

7 Again, we consider the three basic characteristics required for candidate models,
8 as suggested for the univariate case, that is: 1) if no initial velocity exists, the model
9 should reduce back to the normal model from Winter & Yin (2010, 2011); 2) the initial
10 velocity is proportional to the shift in the probability mass; and 3) the mode of the model
11 distribution is identifiable. In the two dimensional case, we consider two alternative
12 properties of candidate models. Let $f_m(s)$ be the function describing the movement
13 probability surface across space (s) for model m . First, the model should exhibit
14 reflectional symmetry about the AoM; defined as:

$$15 \quad f_m(s) = f_m(r_{AoM}(s)) \quad [9]$$

16 where r_{AoM} signifies a reflection along the line defined by the AoM . For most objects,
17 moving in unconstrained space, turning left and right are equally probable. For objects
18 moving along a network turning probabilities may favor left or right turns in specific
19 scenarios.

20 The second consideration is the structure of the resulting distribution. This
21 consideration arose after experimentation with multiple candidate models that seemed
22 reasonable, but exhibited differing resultant shape characteristics. We can examine the
23 structure of $f_m(s)$ to examine symmetry, but also discuss how well the shape of $f_m(s)$

1 aligns with boundaries proposed by Kuijpers et al. (2001). The multivariate skew-normal
2 distribution (Azzalini and Dalla Valle 1996) offers a potentially useful model for
3 modeling future movement probabilities in the spatial plane (i.e., bivariate skew-normal
4 model – Figure 4a). The bivariate skew-normal uses the same three parameters as the
5 univariate skew-normal, replacing scalar values by their multidimensional vector/matrix
6 alternatives, where $\boldsymbol{\zeta}$ is a location vector, $\boldsymbol{\Omega}$ is a scale/covariance matrix, and $\boldsymbol{\alpha}$ is a
7 skewness vector. Again using the proposed alternate parameterization (Arellano-Valle &
8 Azzalini, 2008) one could attempt to relate these parameters to the moments of the
9 bivariate skew-normal distribution, similar to the univariate case. However,
10 parameterizing the bivariate skew-normal is extremely difficult. Recall that we used
11 numerical methods to solve for ζ in the univariate case, which become intractable for the
12 bivariate situation. Further, in the bivariate case the scale/covariance matrix induces
13 assymetries into the model by interrelating the scale and skewness parameters (Arellano-
14 Valle and Azzalini 2008) and therefore would not satisfy the reflectional symmetry
15 property we desire. The absence of symmetry suggests that the bivariate skew-normal
16 distribution may not be useful in this particular application. A seemingly logical
17 alternative would be to model the movement of the object as two independent SN_1
18 distributions (Figure 4b), one for movement in the X direction and one for the Y
19 direction. However, when the magnitude of $v_x \neq v_y$ this form of a model also introduces
20 similar unwanted assymetries in $f_m(s)$, and therefore does not satisfy the reflectional
21 symmetry condition.

22 < approximate location Figure 4 >

1 Given our success at implementing the univariate skew-normal, a potential
2 bivariate skew-normal model would include the product of a skew-normal aligned with
3 the AoM and a normal model aligned with the A+M (Figure 4c). The selection of the
4 normal for the A+M is to satisfy the symmetry requirement, although any symmetric
5 distribution could be accommodated here. The use of the normal distribution here
6 however ensures that we satisfy criterion 2); that the model reduces to that of Winter &
7 Yin in the absence of initial velocity.

8 Alternatively, we propose the use of two univariate skew-normal distributions
9 aligned at 45° of either side of the AoM (Figure 5). The motivation for choosing this
10 formulation is based on repeated experimentation with two independent SN₁
11 distributions. Based on this orientation it can be shown that the initial velocity (along the
12 AoM) can be decomposed into two equal and orthogonal vectors along these
13 corresponding axes. Given an object located at the origin with an initial velocity in
14 direction θ (i.e., θ from the horizontal axis) it is trivial to compute the rotated coordinate
15 system (see Figure 5). Under this rotated coordinate system, the initial velocity will be
16 identical in the rotated axis (x' and y') and computed by:

17
$$v_{x'} = v_{y'} = \sqrt{\frac{v^2}{2}} \quad [10]$$

18 Where x' and y' are the rotated coordinates for two orthogonal axes taken to be 45° from
19 the AoM. Based on this model we can construct a bivariate skew-normal as the product
20 of two identical univariate skew-normal distribution aligned at 45° from the AoM. As can
21 be seen in Figure 4d, this model accommodates all of the requirements of a candidate
22 model.

23 < Approximate location Figure 5 >

1 Unlike with random movement where a strong foundation of theory exists for
2 using the bivariate normal distribution for modeling future movement probabilities (e.g.,
3 Pearson, 1905; Skellam, 1951), no general theory exists for deriving future movement
4 probabilities for kinetic movements. Thus, we chose to further evaluate only the rotated
5 skew normal model, based on qualitative assessment and initial data-driven comparisons
6 between models. Based on our observations and trials we found the rotated skew-normal
7 model provided better alignment with the kinetic time geographic boundaries (Kuijpers
8 et al., 2011; see also Figure 6), but also showed better agreement with movement data
9 based on initial tests. However, the skew-normal / normal model and rotated skew-
10 normal models generate rather similar $f_m(s)$ surfaces (i.e., Figure 4 c and d), and a more
11 thorough investigation of the differences between the models is warranted. From here
12 forward, the rotated SN model (with two axis at 45° from the AoM – Figure 4d) will be
13 implemented and referred to as the SN-model.

14 < Approximate location Figure 6 >

15 2.3 – Model Discussion

16 The model we have proposed is impacted by the assumptions necessarily made to
17 solve the system of equations associated with the skew-normal parameters (i.e., equations
18 [3] to [8]). The first assumption is that the skewness parameter (γ) is proportional to the
19 ratio of the objects current velocity – v_t to v_{max} (i.e., in [4]). Setting the skewness to the
20 ratio of v_t to v_{max} is logical as this bounds γ on $[-1, 1]$, which is the natural range for this
21 parameter. However, the relationship between initial velocity (defined here using the
22 ratio of v_t to v_{max}) and γ may be non-linear and alternative definitions of [4] may be
23 warranted provided they maintain γ on the range $[-1, 1]$. For instance, here we ignore the

1 effect of acceleration (Kuijpers *et al.* 2011), an integral component of object kinetics, in
2 our model definition. A more complete model would include the effect of acceleration on
3 γ and on the variance component (ω). Thus, the proposed skew-normal model represents
4 a first step *towards* a kinetic-based probabilistic time geography, with further
5 developments necessary to adequately factor in kinetic effects associated with
6 acceleration, and generate the appropriate theory.

7 The second assumption we make is on the variance parameter in [6], where
8 existing theory from Winter & Yin (2010, 2011) suggests that at three standard deviations
9 the pdf should equal the time geographic boundary of movement (i.e., $v_{max} \times \Delta t$). Use of
10 this formulation for σ^2 means that in the absence of initial velocity the model reverts to
11 that proposed by Winter & Yin, a property of the model we intended to maintain. For
12 moving objects, increased model skewness and deviation away from the Winter & Yin
13 model occurs as a result of a faster relative initial velocity, or a finer sampling interval.
14 Using the definition in [5] and keeping variance constant, it can be shown that at higher
15 levels of observed skewness the scale parameter (ω), which roughly describes the width
16 of the skew-normal distribution, will be smaller in magnitude than with a lower level of
17 skewness. A smaller width associated with increased initial velocity is a positive result in
18 light of what we might expect with movement situations (i.e., lesser movement
19 opportunities with increased initial velocity – Kuijpers *et al.*, 2011) and further evidence
20 that the proposed model is suited to movement applications. A lingering issue with the
21 Winter & Yin model is probability surfaces defined beyond the physical limits imposed
22 by time geography. Winter & Yin (2011) use the classical time geographic boundaries in
23 order to truncate the model distribution. Similarly, here it would be appropriate to

1 truncate the SN model surfaces using the kinetic boundaries defined by Kuijpers et al.
2 (2011; see also Figure 6).

3 The final assumption we make in the model is given by [8]. Here we assume that
4 the most likely location of future movement (the mode of the resulting two-dimensional
5 surface) is at the location (Δt into the future) associated with unchanging speed and
6 direction by the object. By assuming that moving objects are *most likely* to maintain both
7 speed and direction, the SN model is founded on fundamental rules from motion-based
8 physics (i.e., Newton's first law of motion). This assumption is also apparent in models
9 used to match movement data (e.g., GPS traces) to road networks (e.g., Krumm,
10 Letchner, & Horvitz, 2007). However, the assumption that movement speed and direction
11 are most likely to be constant and unchanging may not hold as Δt increases (e.g., in [8]),
12 however there may be some psychological factor that suggests this relationship is
13 approximately true. In ecology, the tendency of organisms to continue moving in the
14 same direction is termed *persistence* (Othmer *et al.* 1988). In most cases this is unlikely
15 to be related to physical kinetics, but rather other underlying motivations, such as
16 migratory phases, or habitat requirements. It may be useful to consider a persistence-
17 based definition of motion in ecological examples to more appropriately factor in these
18 types of properties of wildlife movements. This would allow kinetic-based ideas from
19 time geography to be included with more coarsely collected wildlife movement datasets
20 (i.e., those with sampling intervals of minutes to hours).

21 **3 Case Study**

22 *3.1 – Data*

1 We have attempted to evaluate the proposed SN model using a combination of
2 simulated and real-world movement datasets (Table 1; Figure 7). The first dataset is a
3 random walk. Similar random models have been suggested by early ecologists as null
4 models for organism movement (Skellam 1951). The second dataset is a correlated
5 random walk. Correlated random walk models are considered one of the best models for
6 the movements of wildlife (Kareiva and Shigesada 1983, Turchin 1998), and commonly
7 used to simulate movement data for method testing (Nams 2005, Börger *et al.* 2008,
8 Long and Nelson 2012). The first empirical dataset used is Caribou data tracking the
9 movement of a single caribou across northern British Columbia over the course of a
10 single year. Location fixes were obtained at a sampling interval of $\Delta t = 4$ hour, using a
11 VHF telemetry system resulting in minimal missing fixes. The second empirical dataset
12 is a GPS track of a commuter cyclist. Cycling data were recorded using a commercial,
13 handheld GPS set to a sampling interval of $\Delta t = 5$ seconds. The final empirical dataset is
14 generated using sport-specific GPS units (GPSports, Fyshwick, Australia) from athletes
15 participating in an ultimate frisbee game. Here GPS relocations of an athlete are collected
16 at a sampling interval of 5 Hz ($\Delta t = 0.2$ s), representing an extremely detailed dataset on
17 individual movement. This sports data has been previously explored in Long &
18 Nelson(2013), in the context of measuring dynamic interactions in player movements.

19 < approximate location Table 1 >

20 < approximate location Figure 7 >

21 3.2 – *Methods*

22 3.2.1 – *Model Set-up*

1 Movement datasets can be used for examining predictive movement models by
2 attempting to predict successive movement fixes based on the previous fixes. In order to
3 do this, we compare the observed location of each fix with the modeled probabilities
4 obtained from either the Winter & Yin model or the SN model. That is, for each fix i in a
5 trajectory we compute two probability surfaces $f_{W\&Y}(x)$ and $f_{SN}(x)$ (e.g., figure 6) that can
6 be used to predict, probabilistically, future movement locations (i.e., fix $i+1$). We extract
7 the observed fix probability from both the Winter & Yin and SN models, along with the
8 maximum observed probability in order to evaluate the two models.

9 3.2.2 – Model Evaluation

10 It is useful to evaluate the predictive ability of the model by examining how well
11 the predictive model aligns with the observed movement data. Typically, one would use a
12 measure of, in this case spatial, distance (e.g., $\|\text{observed} - \text{expected}\|$) to quantify this
13 agreement. Given that we use the mode explicitly in our derivation of skew-normal
14 models (which is not necessarily equivalent to the expected value) we suggest some
15 alternative measures of model agreement.

16 When one model is a special case of another, as in our situation where the normal
17 model is a special case of the SN-model, the likelihood ratio of the two models can be
18 used as a comparison statistic (Kalbfleisch 1985). Owing to its mathematical properties,
19 the natural logarithm of this ratio, termed the log-likelihood ratio is routinely
20 implemented:

$$21 \Lambda_i = \ln \left(\frac{p_a(x_i)}{p_b(x_i)} \right) \quad [11]$$

22 here Λ_i is the log-likelihood ratio for observation i , and $p(x_i)$ is the modeled probability
23 (for model a or b) at observation i . Positive values favor the model a , while negative

1 values favor the model b , values near 0 signify that both models perform equally. In our
 2 examples, model a is the normal model from Winter & Yin (2010, 2011) and model b is
 3 the skew-normal (SN) model incorporating object kinetics. As a result, $\Lambda_i < 0$ indicate the
 4 SN model provided a better fit to the data, while $\Lambda_i > 0$ indicate the Winter & Yin model
 5 demonstrates better agreement. We plot the Λ_i of a particular movement dataset as a
 6 time-series to examine temporal trends in model differences and report the mean values ($\bar{\Lambda}_i$).
 7 Further, a global measure of agreement, the log-likelihood ratio statistic, can be
 8 computed as:

$$9 \quad \text{LLR} = -2 \sum \Lambda_i \quad [12]$$

10 where LLR is the log-likelihood ratio statistic, which is approximated by a chi-square
 11 distribution, with degrees of freedom (df) equal to the difference in the free parameters in
 12 model a and b . In our case, model a is the Winter & Yin model and contains 1 free
 13 parameter; while model b is the SN model and contains 3 free parameters. Therefore, the
 14 d.f. for the LLR test statistic is $3 - 1 = 2$. We use LLR to test for whether the use of the
 15 more complex SN model provides a significant improvement (with $\alpha = 0.01$) over the
 16 Winter & Yin model.

17 To further examine the agreement of the models with the data, we define a
 18 statistic that compares the observed probability for movement i as a ratio of the maximum
 19 modeled probability (the mode of the predictive surface). Termed the predictive
 20 probability, the statistic takes the form:

$$21 \quad PP_{k,i} = \frac{p_k(x_i)}{p_k(\hat{\mu}_i)} \quad [13]$$

1 Where $PP_{k,i}$ is the predictive probability of the k^{th} model for observation i . The numerator
2 is simply the observed probability from the model at observation i . This value is then
3 taken as a ratio of the observed maximum probability (expected value – or mode) of the
4 model, denoted $p_k(\hat{\mu}_i)$ which is used here to appropriately scale values. The ratio defined
5 by [11] can be thought of as a performance measure of the model at each data point, with
6 values closer to 1 signifying that the data and model show good agreement, while values
7 near 0 suggest the model and data are not well aligned. The mean values (PP_k) are
8 reported for each model and a pairwise t -test (with $\alpha = 0.01$) was used to examine
9 whether the evaluative measure ($PP_{k,i}$) differs significantly between the two models.

10 With these five datasets, we have differing expectations of SN model performance
11 when compared with the existing Winter & Yin model. Given that the model of Winter &
12 Yin is based on random walks, we expect the Winter & Yin model to perform better with
13 the random walk dataset. With the correlated random walk dataset we might expect the
14 SN model provide a better agreement, although decreasing the correlation parameter (r –
15 see Table 1) could change this outcome as the correlated random walk would exhibit
16 more random-like behavior. Similarly, wildlife movements are commonly modeled as
17 variations of correlated random walks. We expect that at a relatively coarse sampling
18 interval ($\Delta t = 4$ hr) we will see similar results with the wildlife data as with the correlated
19 random walk. In the cyclist example, we expect that the directed and linear nature of
20 cyclist movement will favor the SN model. Further, the effect of object kinetics is likely
21 dependent on the sampling interval chosen (here $\Delta t = 5$ s), and further decreasing the
22 sampling interval would initiate an even greater influence. Finally, with the athlete
23 movement data we expect the SN model to outperform the existing model due to the

1 relatively high influence of initial velocity in athlete movement and the extremely fine
2 sampling interval ($\Delta t = 0.2$ s).

3 3.3 – Results

4 As expected, for the random walk dataset, the probabilistic time geography model
5 from Winter & Yin (2010, 2011) performed better based on both evaluative tests. The
6 log-likelihood ratio plot (Figure 8a) demonstrates the unpredictable nature of a random
7 walk, with both models outperforming the other in some cases, but on average the normal
8 model of Winter & Yin seems to provide better agreement ($\bar{\Lambda}_i = 0.424$), further
9 supported by the non-significant LLR. For the random walk dataset, the predictive
10 probability of the SN model ($PP_k = 0.456$) is lower than the Winter & Yin model ($PP_k =$
11 0.599), a difference that is highly significant (Table 2). However, both values are
12 relatively low, which suggests that neither model is particularly adept at predicting
13 successive locations of this particular random walk dataset.

14 < approximate location Figure 8 >

15 Similarly, as expected with the correlated random walk, the SN model
16 outperformed the model of Winter & Yin using both visual and statistical tests. As can be
17 seen in the log-likelihood ratio plot (Figure 8b), the difference between the two models in
18 the correlated random walk is similar but opposite than the random walk ($\bar{\Lambda}_i = -0.179$). A
19 significant LLR = 359 suggests that the SN outperforms the Winter & Yin model. With
20 the correlated random walk, the predictive probability ($PP_k = 0.682$) of the SN model is
21 higher than the Winter & Yin model ($PP_k = 0.618$), a difference that is significant (Table
22 2).

1 Plotting the Λ_i from the caribou dataset (Figure 8c) demonstrates that, for the
2 most part, the Λ_i values are near 0. With the caribou example $\bar{\Lambda}_i = 0.0148$, an indication
3 that the model from Winter & Yin slightly outperforms the SN model. However, during
4 specific intervals the SN model outperforms the Winter & Yin model (e.g., the interval
5 occurring in late May). These periods correspond with more active caribou movements
6 associated with annual migration phases. When the caribou is making extensive
7 movements the SN model may be superior, but during low movement phases the two
8 models perform similarly. The LLR indicates that indeed there is no significant
9 advantage of choosing the more complex SN model over the simpler model of Winter &
10 Yin. The test comparing the $PP_{k,i}$ of each model for the caribou dataset revealed that, on
11 average, the SN model has lower predictive probability ($PP_k = 0.958$) than the Winter &
12 Yin model ($PP_k = 0.973$) for this dataset, a small difference, but one that is still
13 significant (Table 2).

14 From the plot of the Λ_i for the cyclist dataset (Figure 8d) it is clear that during
15 specific intervals the SN model demonstrates better agreement (negative Λ_i values).
16 However, at other instances the two models perform identically (i.e., when $\Lambda_i = 0$). Here
17 the cyclist has stopped moving, and in the absence of an initial velocity the two models
18 are equivalent, thus $\Lambda_i = 0$. With the cyclist dataset, $\bar{\Lambda}_i = -0.877$, which suggests that the
19 SN model outperforms the Winter & Yin model, further supported by the significant LLR
20 = 430. A $PP_k = 0.945$ was observed with the SN model, while a much lower $PP_k = 0.548$,
21 was found with the Winter & Yin model, a difference again found to be highly significant
22 (Table 2).

1 The results from the athlete dataset are similar to those from the cyclist dataset.
2 During specific mobile periods the SN model shows better agreement, while during other
3 periods (of stationary behaviour) the two models are similar (Figure 8e). The fact that $\bar{\Lambda}_i$
4 = -0.701 again suggests that the SN model demonstrates better agreement with this
5 dataset, supported by a highly significant LLR = 401. The predictive probability test
6 confirms this observation with $PP_k = 0.949$ for the SN model and $PP_k = 0.650$ for the
7 Winter & Yin model, a highly significant difference (Table 2).

8 **4 - Discussion**

9 We have used two simulated examples along with three real-world datasets to
10 demonstrate the usefulness of the SN model for future movement possibilities in a time-
11 geographic framework. From these examples it is clear that with applications involving a
12 relatively high relative initial velocity (i.e., fast moving objects, with finely sampled
13 movement data), the SN model for probabilistic time geographic proposed here is a far
14 more useful predictor of future movement probabilities than the existing definition based
15 solely on random movement.

16 As discussed by Kuijpers et al. (2011), ignoring object kinetics may be reasonable
17 when estimating broad-scale patterns from finely sampled movement data; for example,
18 when looking at long-term transportation trends. Similarly with coarsely sampled
19 movement data the physical kinetics of movement will not be relevant. For instance, data
20 collected by legacy radio-tracking systems of wildlife use sampling frequencies in the
21 order of hours to days. However, the development of kinetic-based time geography has
22 clear merit in applications where object kinetics are relevant in the construction of time
23 geographic volumes. Such applications include the analysis of finely sampled wildlife

1 movement data (Cagnacci *et al.* 2010), human powered movements, such as by athletes
2 (this paper), and the movements of vessels such as ships and airplanes (Knighton and
3 Claramunt 2001), as well, the role of kinetics can be clearly demonstrated when
4 examining automobile trajectories (Yu and Kim 2006).

5 Wildlife tracking systems are now being equipped with real-time data transfer
6 mechanisms in order to monitor wildlife movements in real-time (Urbano *et al.* 2010).
7 These systems can be used to guide management strategies (e.g., forest harvesting) in
8 important conservation areas based on the location of wildlife (Dettki *et al.* 2004). Here
9 the proposed SN model could be used to improve movement predictions and guide
10 conservation strategies by identifying, probabilistically, specific areas of concern. Video
11 tracking systems are also commonly used to derive movement data of multiple target
12 objects in a fixed spatial domain (e.g., athletes on a playing surface, Liu *et al.*, 2009; Lu,
13 Okuma, & Little, 2009). With video tracking, movement trajectories are often interrupted
14 by visual occlusions, and a single trajectory will become divided into numerous segments
15 (Liu *et al.* 2009, Lu *et al.* 2011). The SN model could also be useful as a tool for
16 connecting trajectory segments in multi-object video tracking systems. Another area of
17 spatial research that is rapidly expanding is the development of location based services
18 (Raper *et al.* 2007). Location based services leverage a client's location through a
19 location aware device (e.g., GPS embedded in a cell-phone) in order to tailor services to
20 clients based on location. Popular examples include restaurant locating or real-time
21 navigation applications on a smart-phone. In such applications, the SN model could
22 improve spatial locating or preference selection by incorporating the motion of the client,
23 especially if they are travelling in a fast moving vehicle such as a car.

1 For many movement applications researchers are interested in extracting patterns
2 from datasets where movement is confined to a (known) travel network (e.g., Miller &
3 Wu, 2000). In these situations the spatial domain cannot be represented as an open two-
4 dimensional plane, but rather as a set of connected network *links* that facilitate essentially
5 one-dimensional movement within the spatial plane. Turns can occur along network
6 links, but primarily at *nodes*, where movement may proceed in one of multiple directions.
7 The framework we have introduced for modeling kinetic-based movement probabilities
8 can still hold in this situation (e.g., Figure 9). Along network links the univariate skew-
9 normal formulation can be used in lieu of the two-dimensional model. At network nodes,
10 the probability density beyond the node can be divided between the available links based
11 on individual node turning probabilities that may reflect pre-determined preferred route
12 choices, and even turning times. A hybrid one-dimensional model draws on the
13 calculations already being used in network analysis algorithms for computing travel times
14 along street networks.

15 < approximate location Figure 9 >

16 Other models for modeling movement probabilities in time geography also exist.
17 Miller and Bridwell (2009) propose field-based time geography where movement
18 probabilities are defined using a movement cost surface. Field-based time geography
19 represents the combination of time geography theory with common GIS operations, (i.e.,
20 those used in least-cost path analysis, Douglas, 1994). Downs (2010) has introduced
21 ideas from time geography into kernel density estimation (commonly used in the study of
22 wildlife movement). Downs replaces the traditional circular kernel (e.g., Gaussian,
23 quartic) with the potential path area from time geography (Figure 1b) and computes a

1 density surface representing the probability an object visits a given location (termed a
2 utilization distribution). Time geographic kernel density estimation can be used to define
3 the interior structure of the potential path area, and has since been extended to work with
4 network-based applications (Downs and Horner 2012).

5 How to model movement probabilities has also been examined in the context of
6 wildlife movement ecology. Horne et al. (2007) have derived a similar probabilistic
7 surface to the Winter & Yin model based on the notion of a Brownian bridge (random
8 walks connected by two end points). Benhamou (2011) has suggested that biased random
9 bridges represent a more suitable model for such movement and has developed a biased
10 random bridge movement model. Both the Brownian bridge and biased random bridge
11 utilize a bimodal distribution for modeling movement probabilities between two fixed
12 locations, which effectively models movement probabilities within the potential path
13 area. Winter & Yin (2010) model movement locations in the space-time prism where
14 movement probabilities are the result of unimodal distributions computed for slices of the
15 space-time prism. Computing the integral (over time) of the Winter & Yin (2010) model
16 would produce a surface for comparison with the Brownian bridge and biased random
17 bridge, providing novel insight on the differences and similarities between these
18 approaches.

19 **5 - Conclusion**

20 We quantify movement probabilities for the space-time cone from time geography
21 using a formulation that incorporates object kinetics, specifically considering initial
22 velocity. Quantifying the interior structure of time geography volumes is currently an
23 area of active research with different methods relying on various underlying assumptions.

1 The SN modeling approach we describe is useful for studying movement data at fine
2 temporal granularities, or where kinetic properties (physical or otherwise) are expected,
3 but may not be appropriate with coarser temporal granularities or slow moving objects. A
4 time geography that incorporates movement kinetics, both in the calculation of volume
5 boundaries as in Kuijpers et al. (2011), and in the interior structure of those volumes as
6 we describe here, will provide a more powerful, and realistic model for studying object
7 movement when kinetic properties are inherent. Future endeavors will involve extending
8 the SN model to the space-time prism, necessary for evaluating movement datasets where
9 fixes are most appropriately represented as start and end anchor points of prisms. Further,
10 we hope to investigate ways for examining intersection probabilities with the SN model,
11 similar to those proposed by Winter & Yin (2010, 2011), which will allow more
12 sophisticated time geographic questions to be investigated.

13 **Acknowledgements**

14 The authors gratefully acknowledge the British Columbia Ministry of Environment for
15 access to the Caribou telemetry dataset. Also, we thank the University of Victoria
16 Ultimate Frisbee Club for participating in ongoing data collection endeavours, including
17 the athlete data used here. Thanks to H. Miller for discussions on a number of points
18 related to kinetic time geography and to W. Othman for access to the code, and some tips,
19 for computing the kinetic time geography boundaries. The constructive comments of four
20 anonymous reviewers greatly improved the presentation of this manuscript.

21

References

- Arellano-Valle, R.B. and Azzalini, A., 2008. The centred parametrization for the multivariate skew-normal distribution. *Journal of Multivariate Analysis*, 99, 1362–1382.
- Azzalini, A., 1985. A class of distributions which includes the normal ones. *Scandinavian Journal of Statistics*, 12 (2), 171–178.
- Azzalini, A. and Dalla Valle, A., 1996. The multivariate skew-normal distribution. *Biometrika*, 83 (4), 715–726.
- Benhamou, S., 2011. Dynamic approach to space and habitat use based on biased random bridges. *PloS one*, 6 (1), e14592.
- Börger, L., Dalziel, B.D., and Fryxell, J.M., 2008. Are there general mechanisms of animal home range behaviour? A review and prospects for future research. *Ecology letters*, 11 (6), 637–50.
- Cagnacci, F., Boitani, L., Powell, R.A., and Boyce, M.S., 2010. Animal ecology meets GPS-based radiotelemetry: a perfect storm of opportunities and challenges. *Philosophical Transactions of the Royal Society of London. Series B, Biological Sciences*, 365 (1550), 2157–2162.
- Codling, E. a, Plank, M.J., and Benhamou, S., 2008. Random walk models in biology. *Journal of the Royal Society Interface*, 5 (25), 813–34.
- Delafontaine, M., Neutens, T., and Weghe, N. Van De, 2011. Modelling potential movement in constrained travel environments using rough space – time prisms. *International Journal of Geographical Information Science*, 25 (9), 1389–1411.
- Dettki, H., Ericsson, G., and Edenius, L., 2004. Real-time moose tracking: an internet based mapping application using GPS/GSM-collars in Sweden. *Alces*, 40, 13–21.
- Douglas, D.H., 1994. Least-cost path in GIS using an accumulated cost surface and slopelines. *Cartographica*, 31 (3), 37–51.
- Downs, J.A., 2010. Time-geographic density estimation for moving point objects. *LNCS 6292*, 6292, 16–26.
- Downs, J.A. and Horner, M.W., 2012. Probabilistic potential path trees for visualizing and analyzing vehicle tracking data. *Journal of Transport Geography*, 23, 72–80.
- Gonzalez, M.C., Hidalgo, C.A., and Barabási, A.-L., 2008. Understanding individual human mobility patterns. *Nature*, 453, 779–782.
- Gupta, R.C. and Gupta, R.D., 2004. Generalized skew normal model. *Test*, 13 (2), 501–524.

- Hägerstrand, T., 1970. What about people in regional science? *Papers in Regional Science*, 24 (1), 6–21.
- Horne, J.S., Garton, E.O., Krone, S.M., and Lewis, J.S., 2007. Analyzing animal movements using Brownian bridges. *Ecology*, 88 (9), 2354–2363.
- Kalbfleisch, J.G., 1985. *Probability and Statistical Inference*. New York, NY: Springer New York.
- Kareiva, P.M. and Shigesada, N., 1983. Analyzing insect movement as a correlated random walk. *Oecologia*, 56 (2-3), 234–238.
- Knighton, R. and Claramunt, C., 2001. An aeronautical temporal GIS for post-flight assessment of navigation performance. *Transactions in GIS*, 5 (1), 53–66.
- Krumm, J., Letchner, J., and Horvitz, E., 2007. Map matching with travel time constraints. In: *SAE World Congress*. Detroit, MI, April 16-19, 11.
- Kuijpers, B., Miller, H.J., and Othman, W., 2011. Kinetic space-time prisms. In: *19th ACM SIGSPATIAL International Conference on Advances in Geographic Information Systems*. New York, NY: Association of Computing Machinery, 162–170.
- Kwan, M., 1998. Space-time and integral measures of individual accessibility: a comparative analysis using a point-based framework. *Geographical analysis*, 30 (3), 191–216.
- Kwan, M., 2004. GIS methods in time-geographic research: geocomputation and geovisualization of human activity patterns. *Geografiska Annaler. Series B, Human Geography*, 86 (4), 267–280.
- Lenntorp, B., 1999. Time-geography – at the end of its beginning. *GeoJournal*, 48 (3), 155–158.
- Liu, J., Tong, X., Li, W., Wang, T., Zhang, Y., and Wang, H., 2009. Automatic player detection, labeling and tracking in broadcast soccer video. *Pattern Recognition Letters*, 30 (2), 103–113.
- Long, J.A. and Nelson, T.A., 2012. Time geography and wildlife home range delineation. *The Journal of Wildlife Management*, 76 (2), 407–413.
- Long, J.A. and Nelson, T.A., 2013. Measuring dynamic interaction in movement data. *Transactions in GIS*, 17 (1), 62–77.
- Lu, W.-L., Okuma, K., and Little, J.J., 2009. Tracking and recognizing actions of multiple hockey players using the boosted particle filter. *Image and Vision Computing*, 27 (1-2), 189–205.

- Lu, W.-L., Ting, J., Murphy, K.P., and Little, J.J., 2011. Identifying players in broadcast sports videos using conditional random fields. *In: IEEE Conference on Computer Vision, CVPR'11*. 8p.
- Miller, H.J., 2003. What about people in geographic information science? *Computers, Environment and Urban Systems*, 27 (5), 447–453.
- Miller, H.J., 2005. A measurement theory for time geography. *Geographical Analysis*, 37 (1), 17–45.
- Miller, H.J. and Bridwell, S.A., 2009. A field-based theory for time geography. *Annals of the Association of American Geographers*, 99 (1), 49–75.
- Miller, H.J. and Wu, Y.-H., 2000. GIS software for measuring space-time accessibility in transportation planning and analysis. *GeoInformatica*, 4 (2), 141–159.
- Nams, V.O., 2005. Using animal movement paths to measure response to spatial scale. *Oecologia*, 143 (2), 179–88.
- Othmer, H.G., Dunbar, S.R., and Alt, W., 1988. Models of dispersal in biological systems. *Journal of Mathematical Biology*, 26, 263–298.
- Pearson, K., 1905. The problem of the random walk. *Nature*, 72, 294.
- Prager, S.D. and Yu, B., 2005. Contextualized probability for approximation of spatiotemporal data distributions. *In: International Conference on Cybernetics and Information Technologies, Systems and Applications (ISAS CITSA)*. Orlando, FL, 318–322.
- R Development Core Team, 2012. *R: A language and environment for statistical computing*. Vienna, Austria: R Foundation for Statistical Computing.
- Raper, J., Gartner, G., Karimi, H., and Rizos, C., 2007. A critical evaluation of location based services and their potential. *Journal of Location Based Services*, 1 (1), 5–45.
- Skellam, J.G., 1951. Random dispersal in theoretical populations. *Biometrika*, 38 (1-2), 196–218.
- Turchin, P., 1998. *Quantitative analysis of movement: measuring and modeling population redistribution in animals and plants*. Sinauer Associates Sunderland MA. Sinauer Associates.
- Urbano, F., Cagnacci, F., Calenge, C., Dettki, H., Cameron, A., and Neteler, M., 2010. Wildlife tracking data management: a new vision. *Philosophical transactions of the Royal Society of London. Series B, Biological sciences*, 365 (1550), 2177–85.

- Winter, S., 2009. Towards a probabilistic time geography. *In: Proceedings of the 17th ACM SIGSPATIAL International Conference on Advances in Geographic Information Systems - GIS '09*. New York, New York, USA: ACM Press, 528–531.
- Winter, S. and Yin, Z.-C., 2010. Directed movements in probabilistic time geography. *International Journal of Geographical Information Science*, 24 (9), 1349–1365.
- Winter, S. and Yin, Z.-C., 2011. The elements of probabilistic time geography. *GeoInformatica*, 15 (3), 417–434.
- Yu, B. and Kim, S.H., 2006. Interpolating and using most likely trajectories in moving-objects databases. *In: S. Bressan, J. Kung, and R. Wagner, eds. DEXA 2006, LNCS 4080*. Springer-Verlag, 718–727.

Table 1: Two simulated and three real-world datasets used to evaluate the existing probabilistic time geography model with the proposed kinetic-based probabilistic time geography model.

Dataset	Type	n	Δt	V_{max} [†]	Comments
RW	Simulated	1000	-	3.7	simm.brown() function in R package 'adehabitatLT', $h = 1$.
CRW	Simulated	1000	-	3.8	simm.crw() function in R package 'adehabitatLT', $h = 1$, $r = 0.8$.
Caribou	Real	1772	4 hr	0.77 m/s	Caribou tracked via satellite VHF telemetry during 2000.
Cyclist	Real	247	5 s	13.5 m/s	Movements of the first author while cycling; tracked using a commercial GPS.
Athlete	Real	288	0.2 s	7.6 m/s	Ultimate frisbee player, over a 1 minute interval of a training match. Collected using a sport-specific GPS device.

[†] V_{max} estimated from the data following Long & Nelson (2012).

Table 2: Results for each of the five example datasets comparing the SN model against the existing model of Winter & Yin.

	$\bar{\Lambda}_i$	LLR	PP_k (SN)	PP_k (W&Y)	Diff.
RW	-0.184	-848	0.456	0.599	-0.143*
CRW	0.0779	359*	0.682	0.618	0.0642*
Caribou	-0.00643	-52.4	0.958	0.973	-0.0151*
Cyclist	0.381	430*	0.945	0.548	0.396*
Athlete	0.304	401*	0.949	0.650	0.299*

*denotes significant value ($p < 0.01$)

Captions:

Figure 1: Structures originating from Hägerstrand's time geography. a) space-time cone, along with an isochrone – a line of equal movement possibility in the future. b) space-time prism, along with the potential path area – the projection of the prism onto the spatial plane.

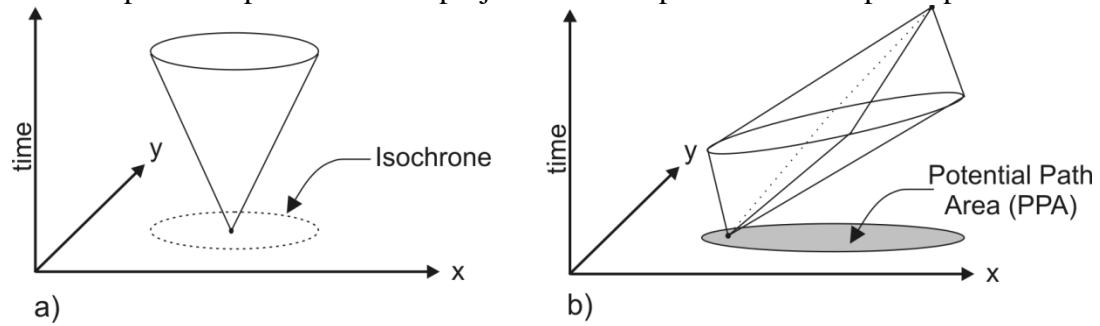
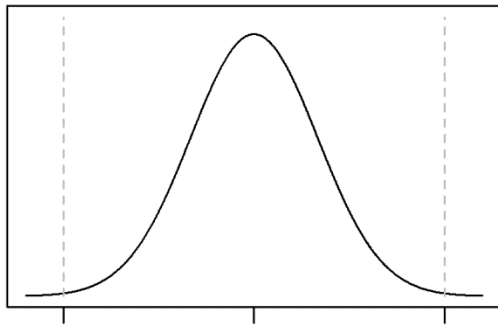
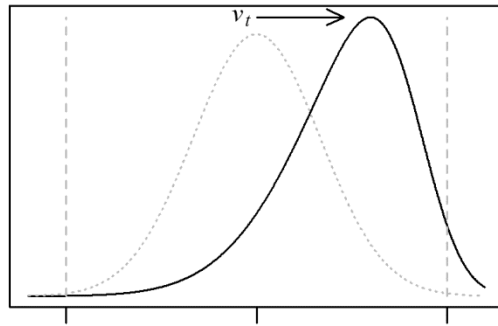


Figure 2: a) Probabilistic time-geography for an object moving in a single dimension; b) Incorporating object kinetics (e.g., v_t); c) and d) Extension of a) and b) to two-dimensions: the spatial plane.



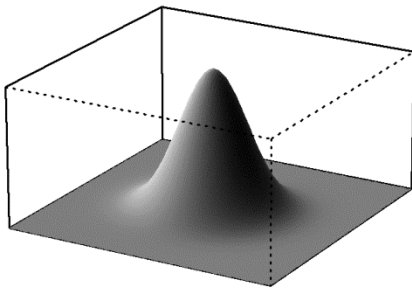
a)

x_t

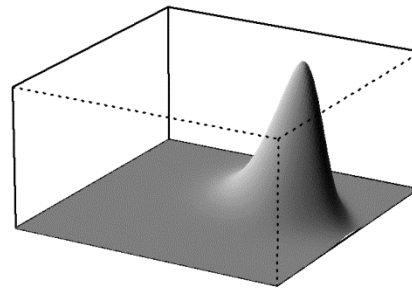


b)

x_t

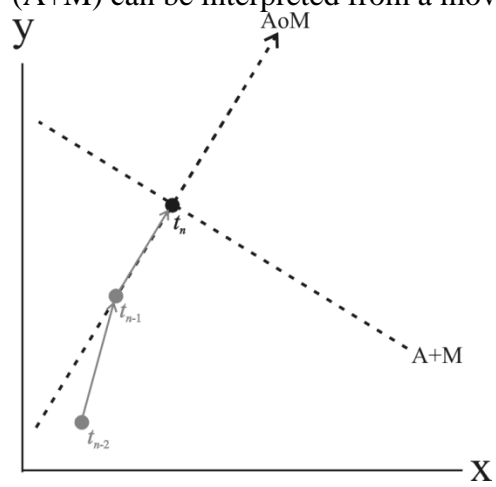


c)



d)

Figure 3: Diagram showing how axis of movement (AoM) and axis perpendicular to movement (A+M) can be interpreted from a movement dataset.



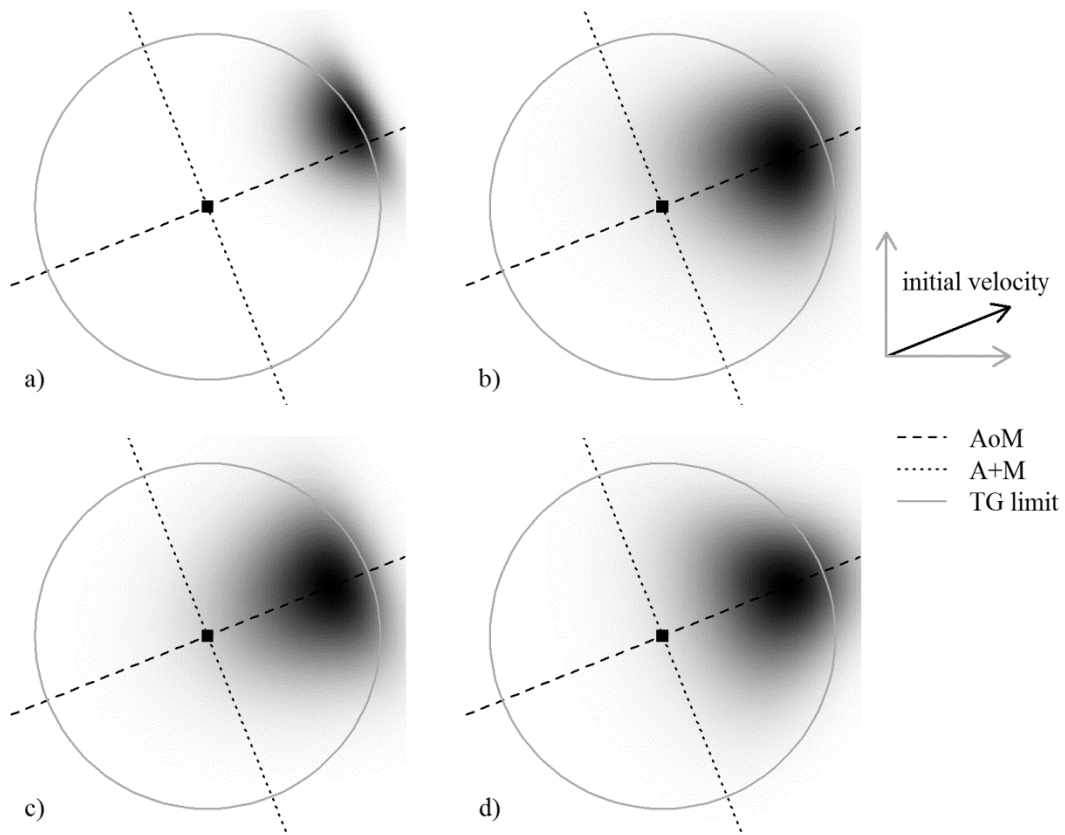


Figure 4: Output probability surfaces, termed $f_m(s)$, for candidate models for predicting future movement possibilities in spatial (2-dimensional) movement applications. a) bivariate skew-normal, b) two univariate skew-normals, aligned with the x- and y-axis, c) univariate skew-normal aligned with the AoM, normal aligned with the A+M, and d) two univariate skew-normals, each aligned at 45° to the AoM, constructed as in Figure 3b.

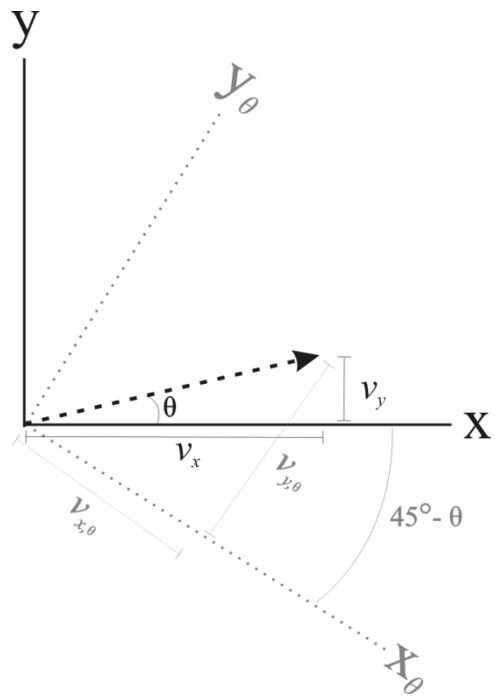


Figure 5: Diagram showing how a rotated coordinate system set up at 45° angles from the AoM can be used to decompose a movement vector into two orthogonal velocities of equal magnitude ($v_{x,\theta}$ and $v_{y,\theta}$).

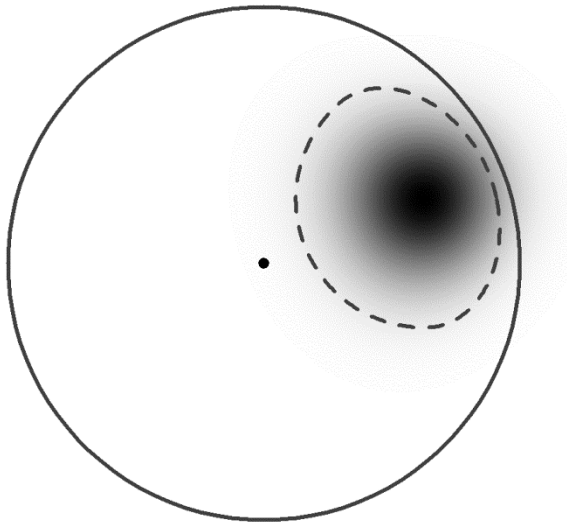


Figure 6: Comparison of proposed SN model (probability surface in greyscale) with kinetic time geographic boundaries (dashed line) defined by Kuijpers et al. (2011). The classic time geographic boundary (large grey circle) is shown for comparison.

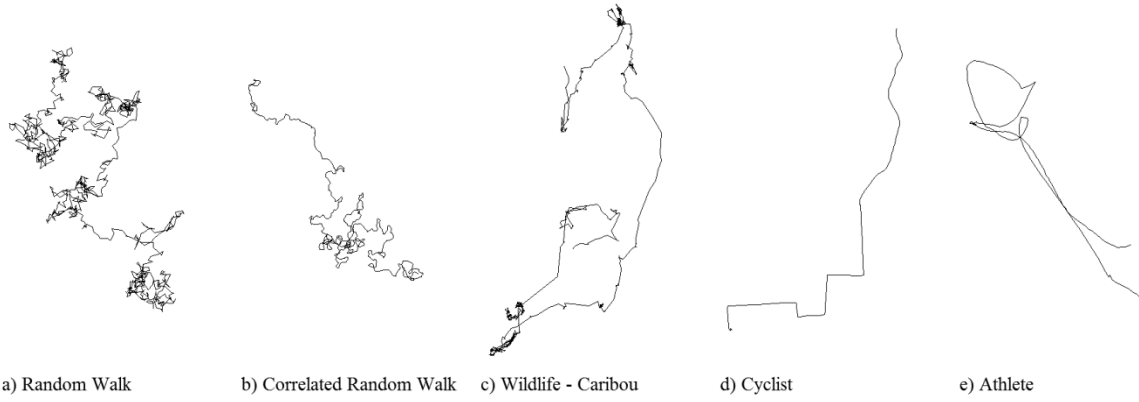


Figure 7: Five example datasets used in evaluating the SN model against the Winter & Yin model; see Table 1 for more details on each dataset.

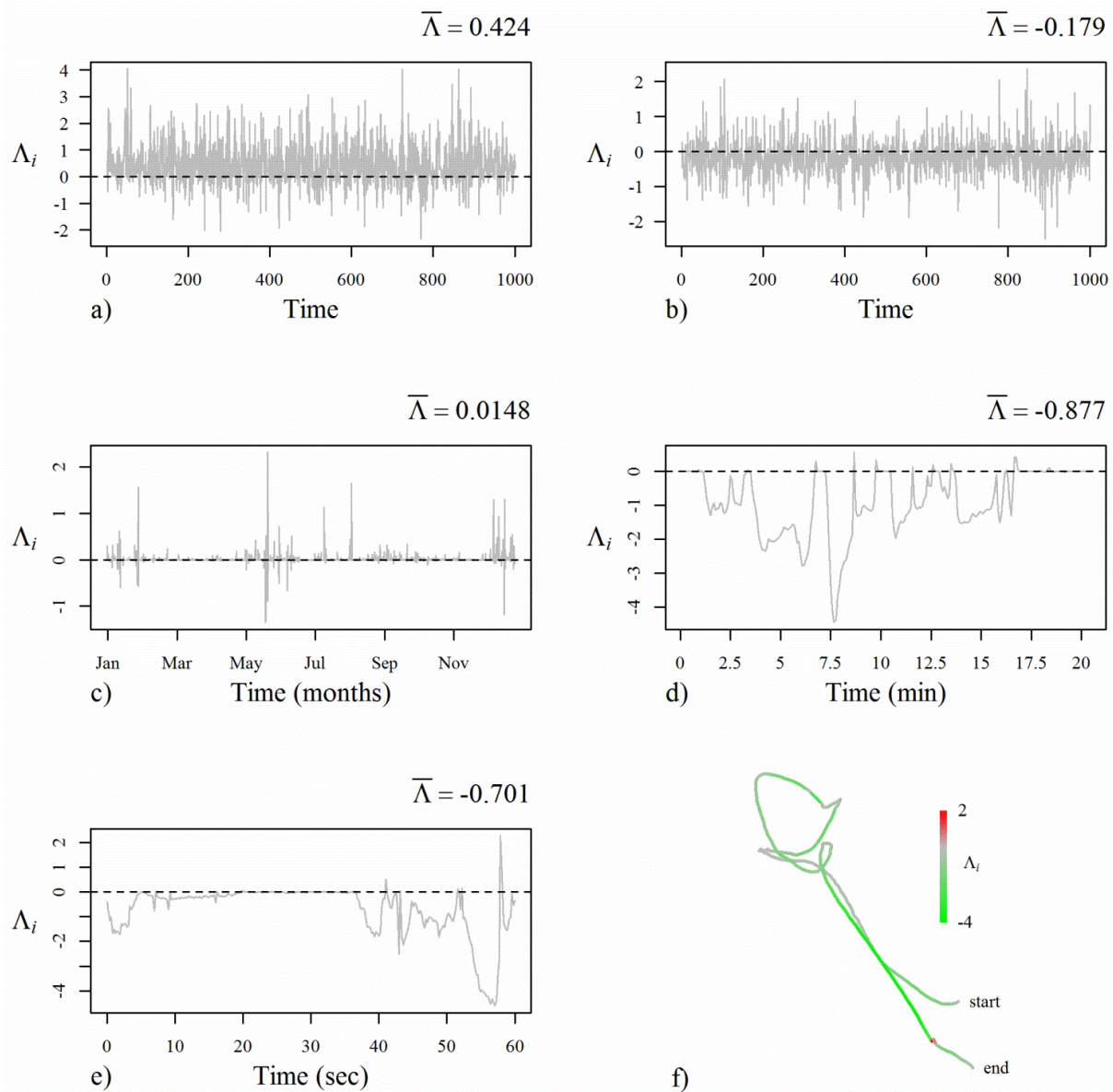


Figure 8: Λ_i results for each of the five sample datasets: a) RW, b) CRW, c) Caribou, d) Cyclist, and e) Athlete. As an example, a map – f), of the Λ_i values associated with the athlete movement dataset can be used to visualize in which parts of the movement trajectory the SN model outperforms the Winter & Yin model (and vice versa). Values for $\Lambda_i > 0$ indicate where the Winter & Yin model agrees better with the movement data, while values for $\Lambda_i < 0$ indicate where the SN model shows better agreement.

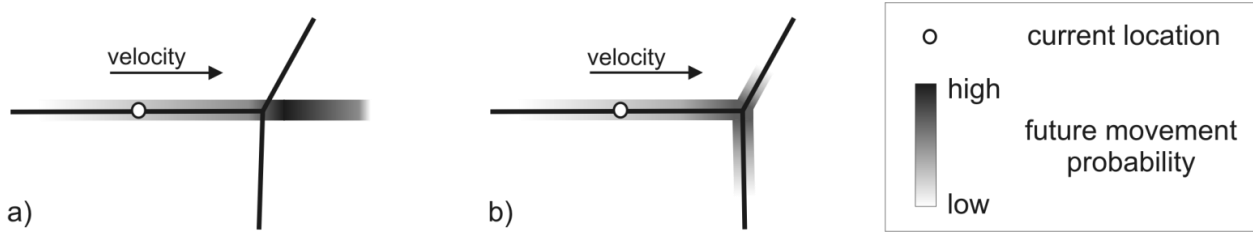


Figure 9: Example of how a hybrid one-dimensional model for kinetic-based probabilities could be applied on a network. a) Kinetic probabilities derived for a moving object along a network link; modeled probabilities extend along the current link, but go beyond the node. b) Turning incorporated at the node, with probability of right turn $>$ left turn.